On the Charge Distribution in Aqueous Poly(styrenesulfonic acid) Solutions. A Small Angle Neutron Scattering Study

J. R. C. van der Maarel,* L. C. A. Groot, J. G. Hollander, W. Jesse, M. E. Kuil, J. C. Leyte, L. H. Leyte-Zuiderweg, and M. Mandel

Department of Physical and Macromolecular Chemistry, Gorlaeus Laboratories, Leiden University, P.O. Box 9502, 2300 RA Leiden, The Netherlands

J. P. Cotton, G. Jannink, and A. Lapp

Laboratoire Léon Brillouin,† CEN-Saclay, 91191 Gif sur Yvette Cedex, France

B. Farago

Institute Laue-Langevin, 156X, 38042 Grenoble Cedex, France

Received June 11, 1993; Revised Manuscript Received September 14, 1993•

ABSTRACT: The partial structure functions and the charge structure function are obtained for aqueous solutions of poly(styrenesulfonate) without excess low molecular weight salt. In the momentum-transfer range $q > 0.1$ Å^{-1}, the structure functions are interpreted in terms of the correlation functions derived from the exact solution of the Poisson–Boltzmann equation in the cell model. The local polymer structure can well be approximated by a rod-like configuration with a rather high linear charge density. The derived charge density is, however, in agreement with the relatively low value of the osmotic coefficient for vinylic polyelectrolytes.

Introduction

The molecular configuration of flexible polyelectrolytes depends on linear charge density and concentration. For instance, the persistence length of a charged chain in solution without added salt is predicted to decrease with increasing polyelectrolyte concentration.[1,2] The polyion form function and distinct pair correlation function (i.e., the polymer structure) of the flexible poly(styrenesulfonate) (PSS) in aqueous solution have been studied by neutron scattering.[3,4] A full description of the polyelectrolyte solution structure, including the effects of the Coulomb interaction, is given by the complete set of monomer–monomer, monomer–counterion, and counterion–counterion partial structure functions.

For a solution containing rod-like DNA fragments (145 base pairs) without added excess salt, all partial structure functions were derived using low-resolution neutron scattering with contrast matching in the water.[5] A self-consistent counterion distribution about the cylindrical polyion can be derived on the basis of the Poisson–Boltzmann equation and the so-called cell model.[6–9] This distribution was found to agree with the experimental data at sufficiently high values of momentum transfer. A similar conclusion was reached on the basis of SAXS intensities, which were fitted to the relevant *combination* of model partial structure functions.[10]

In the present contribution, the partial structure functions of PSS solutions at two different monomer concentrations (i.e., 0.1 and 0.2 monomol/L) will be presented. The counterions are fully deuterated tetramethylammonium ($^{D}TMA^{+}$), and there is no excess simple salt in solution. To obtain these partial structure functions, small angle neutron scattering intensities are measured with different H_2O/D_2O solvent compositions. Finally, the charge structure function is obtained by taking the relevant combination of the partial structure functions.

For *flexible* polyelectrolytes, the requirement for applying the cell model is that the chain can be considered to be *locally* rod-like over a length bearing a sufficiently large number of charges.[9] A chain segment may then be considered as a rigid uniform charged rod situated on the z-axis of a coaxial electroneutral cell. As in case of the DNA fragment solutions, the counterion distribution away from the polymer axis is analytically derived on the basis of the solution of the Poisson–Boltzmann equation. The extent of the momentum-transfer interval is tested in which the polymer can be considered rod-like. The counterion–counterion and monomer–counterion partial structure functions are, in principle, sensitive to the linear charge density, concentration, and distance of closest approach of the counterion to the polymer axis. The present results on PSS are compared to the (less flexible) DNA fragment results.

Theory

The coherent part of the solvent-subtracted intensity of neutron radiation scattered by a polyelectrolyte solution without added simple salt reads[11]

$$I(q) = c[\bar{b}_m^2 S_{mm}(q) + 2\,\bar{b}_m \bar{b}_c\, S_{mc}(q) + \bar{b}_c^2 S_{cc}(q)] \quad (1)$$

Here c is the concentration in monomers per unit volume. The monomer–monomer, monomer–counterion, and counterion–counterion partial structure functions are represented by S_{mm}, S_{mc}, and S_{cc}, respectively. The relatively weights of the different partial structure functions are determined by the scattering length contrasts $\bar{b}_m$ and $\bar{b}_c$ of the monomer and counterion, respectively. These contrast factors can be adjusted by variation of the solvent isotopic H_2O/D_2O composition.[12] For such a solvent mixture, the scattering length contrast $\bar{b}_i$ of the monomers (i = m) or counterions (i = c) is given by

$$\bar{b}_i = b_i - b_s \bar{v}_i/\bar{v}_s \quad \text{with} \quad b_s = X b_{D_2O} + (1 - X) b_{H_2O} \quad (2)$$

where X denotes the D_2O mole fraction. Here b_i and b_s are the scattering lengths of the dispersed particle and solvent, respectively. The corresponding partial molal

* Author to whom correspondence should be addressed.
† Lab. commun CEA-CNRS.
• Abstract published in *Advance ACS Abstracts*, November 15, 1993.

0024-9297/93/2226-7295$04.00/0

Table I. Partial Molal Volumes and Scattering Lengths

	$\bar{\nu}_i$, cm³/mol	b_i, 10^{-12} cm
PSS	114	4.72
^{D}TMA	84	11.6
H_2O	18	−0.168
D_2O	18	1.915

volumes are denoted by $\bar{\nu}_i$ and $\bar{\nu}_s$. These parameters are collected in Table I.

The polyelectrolyte chain is assumed to be a sequence of uniform rigid rods with a length L and radius r_p. Each rod-like segment contains N monomers. The length L may tentatively be identified with the Kuhn segment length, being twice the persistence length L_p. By definition, there is no orientation correlation over a distance larger than the Kuhn segment length. Each rod-like segment is thought to occupy an electroneutral coaxial cell of the same length L but of radius r_{cell}. The cell radius is related to the concentration c according to $cA\pi r_{cell}^2 = 1$ with A being the mean z-axis projected distance between monomers. The distance of closest approach of the counterion center of mass with respect to the polymer central axis is denoted by r_c. This distance r_c is not necessarily equal to the polymer radius r_p, because of the finite counterion size.

In the radial direction the monomer density $\rho_m(r)$ is assumed to be uniform for $0 \le r \le r_p$ and given by $A\rho_m\pi r_p^2 = 1$, and 0 for $r > r_p$. The radial counterion distribution within the cell is obtained from the analytical solution of the Poisson–Boltzmann equation for a uniformly charged cylinder.[6-9] In the longitudinal (z) direction the counterion density is assumed to be uniform. A necessary condition for the application of the Poisson–Boltzmann equation in cylindrical geometry is that the electric field should be close to 0 in a sufficiently wide range near the cell boundary.[8] The model ignores any flexibility of the chain segment. Furthermore, any interactions and/or correlations between different segment cell volumes (intercellular effects) are neglected. Accordingly, the model is expected to have relevance for sufficiently high values of momentum transfer. At the corresponding short distances, the polyelectrolyte can be considered to be rod-like due to the strong electrostatic repulsion between charged beads. Moreover, in this range of momentum transfer, the counterion structure in the immediate vicinity of the polymer is probed.

The partial structure functions for a rod-like segment in cylindrical geometry are evaluated in ref 5. Under neglect of correlations between different cells the structure functions read

$$S_{ij}(q) = \frac{1}{N}\int_0^1 d\mu \left[\frac{\sin(q\mu L/2)}{(q\mu L/2)}\right]^2 P_i(q,\mu)\, P_j(q,\mu) \quad (3a)$$

with $\mu = \cos(\theta)$, θ being the angle between the momentum vector q and the z-axis, and

$$P_i(q,\mu) = 2\pi L \int_0^{r_{cell}} dr\, r J_0(qr(1-\mu^2)^{1/2})\rho_i(r) \quad (3b)$$

The integration over variable μ follows from the isotopic orientation averaging of the cell volume with respect to q, and J_0 denotes the zero-order Bessel function of the first kind. Inserting the step-like radial monomer distribution, eq 3b reduces to (with i = m)[13]

$$P_m(q,\mu) = 2N\frac{J_1(qr_p(1-\mu^2)^{1/2})}{qr_p(1-\mu^2)^{1/2}} \quad (4)$$

The corresponding $P_c(q,\mu)$ has to be calculated using the counterion radial distribution $\rho_c(r)$ obtained from the solution of the Poisson–Boltzmann equation and a numerical integration procedure.

Table II. Concentration, Scattering Length Contrast, and Isotopic Composition

sample	$\bar{m}$, mol/L	$\bar{b}_m$, 10^{-12} cm	$\bar{b}_c$, 10^{-12} cm	X, D_2O
I1	0.096	5.78	12.4	0
I2	0.098	0.22	8.28	0.423
I3	0.101	−4.65	4.69	0.793
I4	0.102	−7.18	2.83	0.983
S1	0.199	5.78	12.4	0
S2	0.200	0.00	8.12	0.444
S3	0.200	−4.69	4.67	0.796
S4	0.200	−7.21	2.81	0.987

The charge structure function S_{zz} is defined by the combination[14]

$$S_{zz}(q) = S_{mm}(q) - 2S_{mc}(q) + S_{cc}(q) \quad (5)$$

In the case of simple electrolyte solutions, S_{zz} obeys the Stillinger–Lovett sum rule[15]

$$S_{zz}(q) = 2q^2/\kappa^2, \quad \text{with} \quad q < \kappa \quad (6)$$

with κ^{-1} being the Debye screening length. In solutions containing polyelectrolytes with a high linear charge density and cylindrical symmetry, the screening length κ^{-1} and, hence, the corresponding limiting behavior of S_{zz} are unknown.

Experimental Section

Sodium poly(styrenesulfonic acid) (NaPSS), degree of polymerization DP = 1300, was obtained from Pressure Chemicals. After dialysis against pure water, the PSS was brought into the acid form by an ion exchange resin. The polyacid was neutralized with fully deuterated tetramethylammonium-d_{12} hydroxide (^{D}TMAOH) to obtain the ^{D}TMA–PSS salt. Two sets of samples were prepared at monomer concentrations $\bar{m}$ = 0.1 and 0.2 mol/L (i.e., $c = 5.98 \times 10^{-5}$ and 12.04×10^{-5} monomers/Å³), and with four different solvent isotopic H_2O/D_2O compositions. The scattering length contrasts have been calculated using eq 2 and the parameters in Table I. The results are collected in Table II. The samples I1–4 and S1–4 will be referred to as samples I and S, respectively. The sample series with four different solvent compositions will be referred to as sample series 1–4.

Neutron scattering experiments were performed using the D17 (samples I, $\bar{m}$ = 0.1 mol/L) and the PACE (samples S, $\bar{m}$ = 0.2 mol/L) diffractometers situated on the cold sources of the high neutron flux reactors at the Institute von Laue-Langevin (samples I) and Laboratoire Léon Brillouin (samples S), respectively. A wavelength of 11 Å was selected. The scattered radiation was measured by a planar square multidetector. For the PACE instrument, the maximum q value was 0.37 Å⁻¹. The D17 planar detector was rotated around the sample, reaching a maximum q value of 0.51 Å⁻¹. Standard quartz sample containers with 0.2-cm (for D_2O-containing samples) or 0.1-cm path length were used. The temperature was controlled at 293 K. The average counting time per sample (i.e., including a reference solvent sample) was approximately 10 and 40 h on the D17 and PACE instruments, respectively. The intensities were put on an absolute scale by normalizing to pure H_2O, and the scattering of the reference solvent sample was subtracted.[16] Finally, the intensities were corrected for a small solute incoherent scattering contribution.

Results and Discussion

The scattered intensities divided by the concentration are displayed vs momentum transfer in Figures 1–4. At very low q values ($q < 0.02$ Å⁻¹) for D_2O-containing samples the intensity increases with decreasing q. This effect is more or less proportional to the D_2O mole fraction. Similar behavior has been observed for solutions containing DNA fragments with ^{H}TMA counterions. Accordingly, the increase at small q seems to be a general "polyelectrolyte"

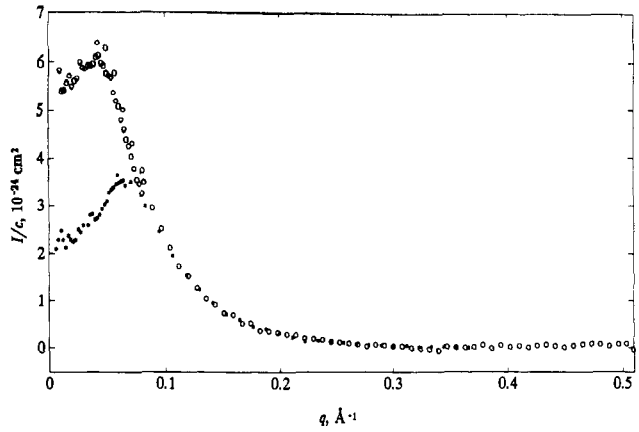

Figure 1. Intensity divided by concentration vs momentum transfer: (O) sample I1; (*) sample S1.

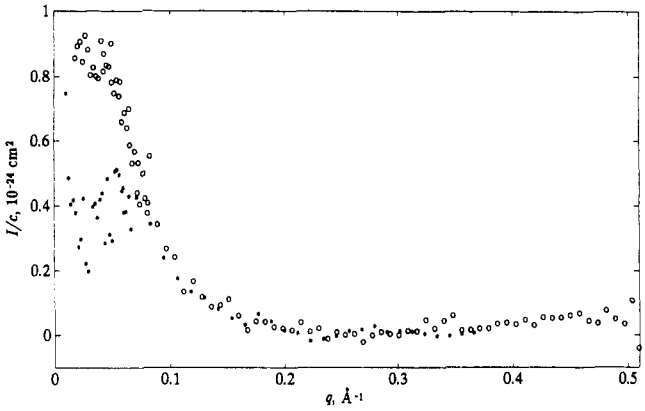

Figure 2. Intensity divided by concentration vs momentum transfer: (O) sample I2; (*) sample S2. The signal is proportional to the counterion structure.

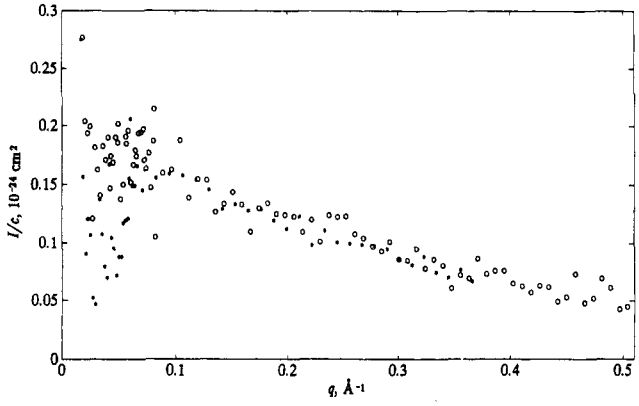

Figure 3. Intensity divided by concentration vs momentum transfer: (O) sample I3; (*) sample S3. In this situation of zero average contrast the signal is proportional to the charge structure.

phenomenon, although, at present, an explanation cannot be given. A number of experimental parameters have been checked, such as D_2O purity, cell path length, pulsed and reactor neutron sources, and different diffractometers. No influence of these various parameters on the low q ($q < 0.02$ Å^{-1}) upturn was observed. As will be shown below, at higher values of momentum transfer, the data are consistent with D_2O mole fraction independent partial structure functions. Accordingly, it is assumed that for $q > 0.02$ Å^{-1} the data are not influenced by this effect.

For sample series 2 (i.e., I2 and S2), the monomer scattering length density is approximately 0 (see Table II). The intensity is then proportional to the counterion structure function. For sample series 3 the monomer and counterion scattering length contrasts have approximately the same absolute value, but opposite sign (zero average

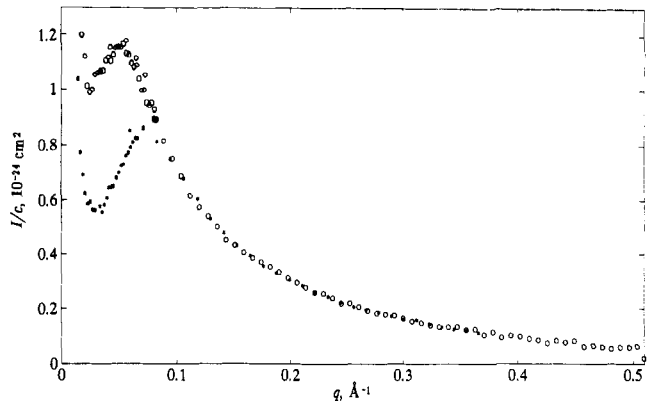

Figure 4. Intensity divided by concentration vs momentum transfer: (O) sample I4; (*) sample S4.

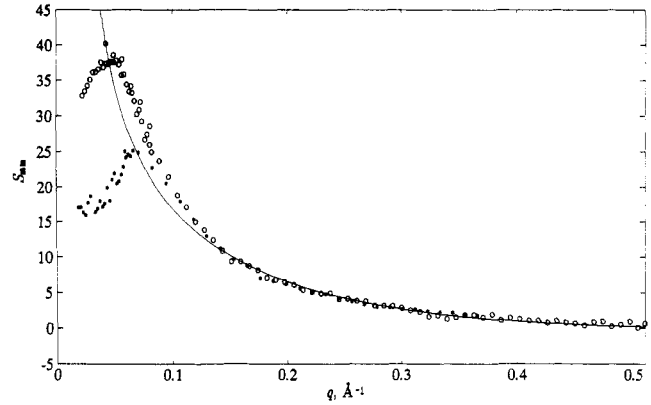

Figure 5. The monomer–monomer partial structure function S_{mm}: (O) 0.1 mol/L I samples; (*) 0.2 mol/L S samples. The solid curve represents the structure function of a uniform rod with $r_p = 5.9$ Å, $L = 150$ Å, and $A = 1.64$ Å.

contrast). In this situation the scattered intensity is directly proportional to the charge structure function. For sample series 1 and 4 the contrast parameters have relatively high values, resulting in a relatively intense scattering. However, for samples I1 and S1 the scattering is dominated by the counterions, whereas for samples I4 and S4 the monomer has the highest scattering length contrast.

Provided that the partial structure functions are independent of the D_2O mole fraction, these functions can be derived according to eq 1 and the scattering length contrasts collected in Table II. Equation 1 is overdetermined, because for each concentration there are four intensities (with different sets of contrast parameters) and three partial structure functions only. Accordingly, the best solutions for $S_{mm}(q)$, $S_{mc}(q)$, and $S_{cc}(q)$ were computed in a least-squares sense using orthogonal factorization.[17] The results are displayed in Figures 5–7. It was checked that for $q > 0.02$ Å^{-1} the derived set of partial structure functions is consistent with the original intensities. The counterion partial structure functions are similar to the intensities of sample series 2, i.e., apart from a scaling factor related to the contrast.

The monomer partial structure function (Figure 5) shows a maximum which decreases in intensity and shifts to higher values of momentum transfer with increasing monomer concentration. At high q values, say beyond $q = 0.1$ Å^{-1}, the structure functions obtained for these two different monomer concentrations coincide. Accordingly, in this range of momentum transfer, interference effects between different polyions are immaterial. Furthermore, at this distance scale ($q > 0.1$ Å^{-1}) a possible concentration-induced change in polyion conformation is not observed.

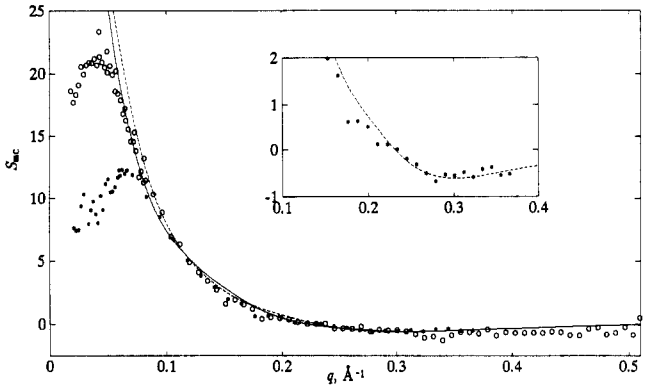

Figure 6. The monomer–counterion partial structure function S_{mc}: (○) I samples; (*) S samples. The curves are drawn according to the cell model calculations. Solid curve: r_c = 9 Å, r_p = 5.9 Å, L = 150 Å, A = 1.64 Å (0.1 mol/L parameters). Dashed curve: r_c = 9 Å, r_p = 6.0 Å, L = 80 Å, A = 1.62 Å (0.2 mol/L parameters). The expanded inset shows the minimum in S samples S_{mc} at $q \approx 0.3$ Å^{-1}.

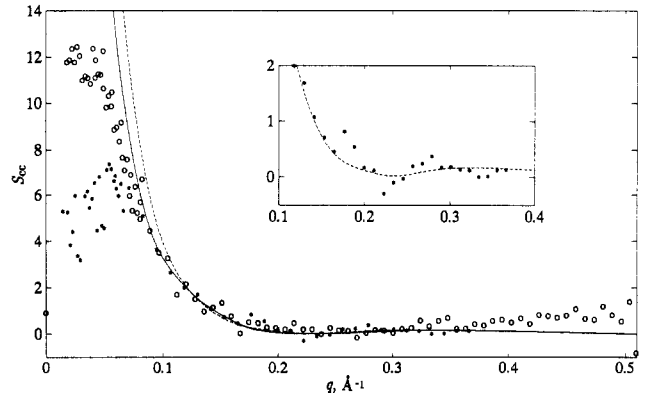

Figure 7. The counterion–counterion partial structure function S_{cc}: (○) I samples; (*) S samples. The curves are drawn according to the cell model calculations. Solid curve: r_c = 9 Å, L = 150 Å, A = 1.64 Å (0.1 mol/L parameters). Dashed curve: r_c = 9 Å, L = 80 Å, A = 1.62 Å (0.2 mol/L parameters). The expanded inset shows the weak oscillation in S samples S_{cc}.

The polyion is assumed to be a sequence of uniform rigid rods. Any correlations between different segments (i.e., both intra- and intermolecular) are neglected. In Figure 5 the solid line represents a nonlinear fit of eqs 3 and 4, in which the polymer radius r_p and the projected mean distance between monomers A were optimized. The fit was performed in the range $q > 0.13$ Å^{-1}. The segment length was fixed at 150 and 80 Å for the I and S samples, respectively. These lengths were calculated using the experimental persistence length obtained by recent neutron scattering experiments on 0.3 mol/L NaPSS[4] and an inverse concentration scaling given by Odijk's expression for the electrostatic contribution.[18] However, it was checked that in the present momentum-transfer range the actual choice of the segment length has only a minor effect on the values of the fitted parameters r_p and A. For the 0.1 mol/L I samples, the optimized value for r_p varied between 6.2 and 5.8 Å for 30 Å < L < 500 Å, and r_p = 5.9 Å for L = 150 Å. The corresponding value for A varied between 1.51 and 1.65 Å for 30 Å < L < 500 Å, and A = 1.64 Å for L = 150 Å. For the 0.2 mol/L S samples a similar behavior was found.

The value for r_p (≈6 Å) is in agreement with the relatively bulky sulfonated benzene side group. The projected mean distance between monomers A (≈1.6 Å) is significantly smaller than the value obtained for the completely stretched cis or trans backbone configuration (i.e., 2.1 or 2.5 Å, respectively). A possible explanation for the relatively short value for A is a helical twist of the polymer backbone. Using the fitted values of r_p and A, the PSS partial monomolal volume can be calculated according to $N_{av}\pi r_p^2 A$. For 30 Å < L < 500 Å, one obtains 105–110 cm^3/mol, in fair agreement with the density result 114 cm^3/mol (Table I).

In the range 0.05 Å^{-1} < q < 0.13 Å^{-1} the deviation of the rigid rod structure function from the experimental data is more pronounced than in the case of the DNA fragment nucleotide structure function at a similar monomer concentration (see Figure 5, ref 5). This might be due to the neglected curvature effects, which are expected to be more important for the more flexible PSS.

The relatively short value for A has a profound effect on the counterion distribution due to the intimately related high linear charge density parameter λ. The latter parameter is defined as the ratio of electrostatic energy between neighboring charges on the chain to thermal energy, $\lambda = e^2/4\pi\epsilon AkT$. At 293 K, for PSS the parameter λ takes the value 4.3. This figure is of the same order of magnitude as the corresponding value for DNA (λ = 4.15). Accordingly, the counterion distribution and, hence, the partial structure functions $S_{mc}(q)$ and $S_{cc}(q)$ are expected to be similar for both the PSS and DNA solutions. Comparison of the present results to the data reported in ref 5 shows that this is indeed the case.

The structure functions $S_{mc}(q)$ and $S_{cc}(q)$ are calculated using eqs 3 and 4 together with the analytical solution of the Poisson–Boltzmann equation.[6-8] In this calculation, the structural parameters L, r_p, and A were fixed at the former values used to describe the monomer structure. For the distance of closest approach of the center of mass of the counterions to the rod central axis, an optimized value r_c = 9 Å was used. The cell model calculations are also displayed in Figures 6 and 7. There is excellent agreement for sufficiently high values of momentum transfer. In this q range, the counterion structure about the polyion is probed. Furthermore, the structure functions of the 0.1 mol/L (I) and 0.2 mol/L (S) samples coincide. Accordingly, in this rather limited molality range, concentration effects on the counterion distribution are of minor importance. For lower q values, the agreement is poor due to the neglect of intercellular and/or curvature effects.

The S sample structure function $S_{mc}(q)$ shows a minimum at momentum transfer $q \approx 0.3$ Å^{-1} (see inset, Figure 6). Unfortunately, as displayed in the inset of Figure 7, the corresponding weak maximum in $S_{cc}(q)$ is not clearly resolved due to the limited experimental accuracy. These extremes are related to the shell-like clustering of counterions about the polyion. It is interesting to note that for DNA solutions the minimum in $S_{mc}(q)$ is shifted to $q \approx 0.2$ Å^{-1}, because of the larger distance of closest approach (r_c = 14 vs 9 Å). The extremes are not observed for the I samples. For the latter samples, at q values > 0.3 Å^{-1}, the structure functions $S_{mc}(q)$ and $S_{cc}(q)$ deviate significantly from the theoretical curves. This can be due to a base-line artifact in the scattering of sample I2 (Figure 2). Another explanation is that for these high values of momentum transfer the details of the molecular structure should be taken into account.

The charge structure function is obtained by combining the partial structure functions according to eq 5. The results are displayed in Figure 8, together with the cell model calculations. For the S samples, at the high q end there is reasonable agreement. The samples I data deviate

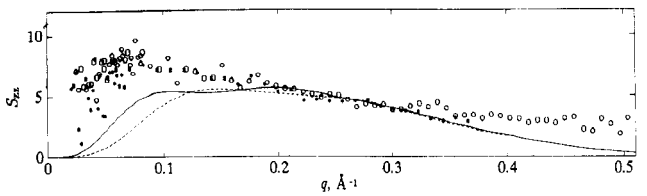

Figure 8. The charge structure function S_{zz} obtained by combination of the partial structure functions: (O) I samples; (*) S samples. The curves are drawn according to the cell model calculations. Solid curve: 0.1 mol/L parameters. Dashed curve: 0.2 mol/L parameters (see Figures 6 and 7).

from the theoretical curve for $q > 0.3$ Å^{-1}. Again, this might be caused by an experimental artifact or the neglect of the detailed molecular structure of the various chemical components. For low q values the agreement is poor. This is due to the neglect of interference and chain flexibility effects, most notably in S_{mm}.

The derived charge structure function is similar to the corresponding function for a solution containing rod-like DNA fragments.[5] The present result is somewhat less intense and extended over a broader momentum-transfer range. This is related to the less extended local charge separation for PSS (due to the smaller value of the polymer radius). In principle, from eq 6 an empirical value for κ^{-1} can be estimated. A clear limiting q^2 behavior in $S_{zz}(q)$ is not observed, because of the poor S/N ratio and the D_2O-induced increase in intensity in the low-q region. However, a lower bound for κ^{-1} can still be estimated from the observed maximum in S_{zz}. For the 0.1 and 0.2 mol/L solutions κ^{-1} takes at least the values 4 ± 1 and 3 ± 1 nm, respectively.

Conclusions

The intensities were measured in absolute units (cm^{-1}), and hence, the derived structure functions are in absolute numbers. In the momentum-transfer range $q > 0.1$ Å^{-1}, the monomer structure agrees with the structure function of a uniform rigid rod. This emphasizes the local rod-like structure, caused by the strong electrostatic repulsion of the charged beads. The short mean projected distance between monomeric units $A = 1.6$ Å results in a 1.7 times higher value of the charge density parameter λ compared to the value corresponding to a fully stretched (trans) chain conformation. This result is in accordance with the relatively low value of the osmotic coefficient ϕ for vinylic polyelectrolytes.[7] For instance, for HPSS solutions at 273 K the osmotic coefficient data agree with the cell model theory for λ is 1.4 times the fully stretched value.[19] In this context it is interesting to note that for the relatively rigid DNA the value for A derived from both colligative properties[7,19] and neutron scattering[5] agrees with the structural value 1.71 Å. Accordingly, it is concluded that PSS does not take its fully stretched local configuration. A possible explanation is a helical twist in the polyion structure, possibly stabilized by stacking of the sulfonated benzene side groups. The obtained value of the polymeric radius $r_p = 6$ Å is in agreement with the size of the relatively bulky side groups. For lower q values ($q < 0.1$ Å^{-1}), the agreement is poor due to the onset of flexibility and, eventually, interference effects between different segments and polyion domains.

The counterion–counterion and counterion–monomer partial structure functions are interpreted using the charge distribution as obtained from the Poisson–Boltzmann equation and the cell model. The calculated structure functions are found to agree with the experimental data for $q > 0.1$ Å^{-1}. The functions S_{mc} and S_{cc} bear some resemblance to the corresponding functions of a DNA fragment solution,[5] due to the similar linear charge density. For both structure functions the best fit yields for the distance of closest approach of the counterion to the polymer central axis $r_c = 9$ Å. This value roughly agrees with the sum of the polymer and the counterion radius, 6 and 3.5 Å, respectively.[20] The minimum in S_{mc} and the weak oscillation (if any) in S_{cc} (0.2 mol/L data) reflect the shell-like clustering of counterions about the polyion. For low q values ($q < 0.1$ Å^{-1}) the agreement is poor. This is clearly due to the shortcomings of the cell model.

The charge structure function was obtained by taking the relevant combination of the partial structure functions. In the PSS (and DNA) polyelectrolyte solutions, the charge structure functions are an order of magnitude more intense compared to the corresponding function of a "simple" electrolyte solution.[21] This is related to the charge separation and counterion accumulation at the polyion interface. At sufficiently high values of momentum transfer, the cell model calculation agrees reasonably with the experimental data. An inaccurate empirical value of the Debye screening length can be estimated from the low q behavior of S_{zz}.

References and Notes

(1) Odijk, T. J. *Macromolecules* **1979**, *12*, 51.
(2) Witten, T. A.; Pincus, P. *Europhys. Lett.* **1987**, *3*, 315.
(3) Nierlich, M.; Boué, F.; Lapp, A.; Oberthür, R. *J. Phys.* (*Paris*) **1985**, *46*, 649; *Colloid Polym. Sci.* **1985**, *263*, 955. Nallet, F.; Jannink, G.; Hayter, J.; Oberthür, R.; Picot, C. *J. Phys.* (*Paris*) **1983**, *44*, 87. Jannink, G. *Makromol. Chem., Macromol. Symp.* **1986**, *1*, 67. Kaji, K.; Urakawa, H.; Kanaya, T.; Kitamura, R. *J. Phys.* (*Paris*) **1988**, *49*, 993.
(4) Boué, F.; Lapp, A.; Cotton, J. P.; Jannink, G. Preprint.
(5) van der Maarel, J. R. C.; Groot, L. C. A.; Mandel, M.; Jesse, W.; Jannink, G.; Rodriguez, V. *J. Phys. II* **1992**, *2*, 109.
(6) Alfrey, T., Jr.; Berg, P. W.; Morawetz, H. *J. Polym. Sci.* **1951**, *7*, 543.
(7) Katchalsky, A. *J. Pure Appl. Chem.* **1971**, *26*, 327.
(8) Mandel, M. *Encyclopedia of polymer science and engineering*, 2nd ed.; John Wiley & Sons, Inc.: New York, 1988; Vol. 11.
(9) Mandel, M. *J. Phys. Chem.* **1992**, *96*, 3934.
(10) Chang, S.-L.; Chen, S.-H.; Rill, R. L.; Lin, J. S. *J. Phys. Chem.* **1990**, *94*, 8025.
(11) Jannink, G.; van der Maarel, J. R. C. *Biophys. Chem.* **1991**, *41*, 15.
(12) Jacrot, B. *Rep. Prog. Phys.* **1976**, *39*, 911.
(13) Jahnke, E.; Emde, F. *Table of functions with formulas and curves*; (Dover Publications: New York, 1943).
(14) Hansen, J.-P.; McDonald, I. R. *The theory of simple liquids*; Academic Press: New York, 1986.
(15) Stillinger, J.; Lovett, R. *J. Chem. Phys.* **1968**, *49*, 1991.
(16) Terech, P.; Volino, F.; Ramasseul, R. *J. Phys.* (*Paris*), *46*, 895.
(17) Matlab Numeric Computation Software, The Math Works Inc., 1991.
(18) Odijk, T. J. *J. Polym. Sci., Polym. Phys. Ed.* **1977**, *15*, 477.
(19) Dolar, D. *Polyelectrolytes, Charged and reactive polymers*; Sélégny, E., Mandel, M., Strauss, U. P., Eds.; Reidel: Dordrecht, 1974; Vol. 1.
(20) Finney, J. L.; Turner, J. *Faraday Discuss. Chem. Soc.* **1988**, *85*, 1.
(21) Jannink, G.; Kunz, W.; van der Maarel, J. R. C.; Calmettes, P.; Cotton, J. P. *Lecture Notes in Physics 415, Complex Fluids, Proceedings of the XII Sitges Conference*; Garrido, L., Ed.; Springer: Berlin, 1993.